Applied Catalysis B: Environmental 84 (2008) 251–261

Contents lists available at ScienceDirect

Applied Catalysis B: Environmental

journal homepage: www.elsevier.com/locate/apcatb

Catalytic oxidation of chlorobenzene over Pd/perovskites

J.-M. Giraudon *, A. Elhachimi, G. Leclercq

Unité de Catalyse et de Chimie du Solide, UMR CNRS 8181, USTL, Bâtiment C3, 59655 Villeneuve d'Ascq, France

ARTICLE INFO

Article history:
Received 14 November 2007
Received in revised form 31 March 2008
Accepted 5 April 2008
Available online 1 May 2008

Keywords:
Chlorinated VOC
Catalytic oxidation
Palladium
Perovskite

ABSTRACT

The catalytic performances of pre-reduced palladium catalysts supported on lanthanum based perovskites $LaBO_3$ (B = Co, Mn, Fe, Ni) were investigated for the total oxidation of chlorobenzene (PhCl; 1000 ppmv) in air. The catalysts were prepared using a wet impregnation technique and Pd-nitrate was used as a palladium precursor. The catalytic performances were compared to those of a reference palladium catalyst supported on a conventional support, namely γ-Al_2O_3. Easiness of chlorobenzene destruction was found to follow the sequence based on the T_{50} values (temperature at which 50% of chlorobenzene was converted into products): $Pd/LaMnO_{3+\delta}$ (243 °C) > $Pd/LaFeO_3$ (270 °C) > Pd/Al_2O_3 (348 °C) > $Pd/LaCoO_3$ (360 °C) > $Pd/LaNiO_3$ (408 °C). Complete conversion of chlorobenzene is reached at ca. 320–500 °C, but at those temperatures substantial amounts of polychlorinated benzenes are formed. *Quasi in situ* XPS studies were monitored on $Pd/LaCoO_3$ and $Pd/LaFeO_3$ after each stage of the global process, namely after calcination, reduction and exposure to the flowing reactive mixture (1000 ppmv PhCl in air) from room temperature to 230 and 310 °C ($Pd/LaFeO_3$) and to 280 °C ($Pd/LaCoO_3$). It was shown that the calcination treatment leads to a palladium which a BE higher than that of PdO and to a $(B/La)_{XPS} < 1$ which attests of a lanthanum enrichment at the XPS surface. After H_2 treatment it was shown that palladium is totally reduced while the B cation is either unreduced (Fe^{3+}) or reduced (Co^{3+} into Co^{2+} and Co^0). In the reactive atmosphere, Pd^0 is progressively (oxi)chlorined while the perovskite network is reconstructed with productions of LaOCl and Co_3O_4. The pre-reduced $Pd/LaBO_3$ are more active than the perovskite alone for PhCl transformation but substantially increase the chlorination rate of PhCl. Among the different catalysts $Pd/LaFeO_3$ shows the best compromise between PhCl oxidation and chlorination rates.

© 2008 Elsevier B.V. All rights reserved.

1. Introduction

The development of efficient catalysts for the total oxidation of chlorinated organic compounds (VOCs) is desirable from the view point of the environment protection. Among the various chlorinated VOCs abatement treatments, catalytic oxidation is a well promising method as it operates at low temperatures and can convert VOCs into harmless compounds [1].

Usually two types of catalysts, noble metal, and transition metal oxides have been used for catalytic oxidation of chlorinated aromatics. The performances of Pt/Al_2O_3 have been investigated for chlorobenzene by van den Brink et al. [2–4]. The major drawback for the application of noble metals for such reaction is the formation of polychlorinated ($PhCl_x$ (x = 2–6)) by-products. However, the activity of noble metals for combustion of chlorinated aromatics is usually higher than for metal oxides. Thereby, supported noble metal catalysts do deserve further research and development [3]. As it is well known that the nature of the support has a great influence on the catalytic properties of the supported noble metal catalysts, the effect of conventional supports was investigated for chlorobenzene total oxidation and it was found that PhCl conversion as well as the congener and isomer distribution differed for various supports [2–4].

In the three-way catalysis it has been previously shown that the use of ceria as support of noble metals, considered as having mobile oxygen, significantly increases the oxidation rate of the pollutants compared to conventional supports [5].

With the regard of such results the objective of this study was to investigate the performances of pre-reduced $Pd/LaBO_3$ (B = Co, Fe, Mn, Ni) in the total oxidation of PhCl (1000 ppmv) by air. The primary characteristic of these catalysts is the association of a noble metal (palladium), well known to activate in an efficient way the VOC with a binary oxide (lanthanum based perovskite) able to give either poor or rich oxygen phases [6]. This series of catalysts

* Corresponding author. Tel.: +33 3 20 43 68 56; fax: +33 3 20 43 65 61.
E-mail address: jean-marc.giraudon@univ-lille1.fr (J.-M. Giraudon).

0926-3373/$ – see front matter © 2008 Elsevier B.V. All rights reserved.
doi:10.1016/j.apcatb.2008.04.023

has already been used for the total oxidation of toluene and the surface states of the $Pd/LaFeO_3$ and $Pd/LaCoO_3$ catalysts have been studied in details by XPS after each step of the global process [7]. The best catalyst was found to be $Pd/LaFeO_3$. No correlations were found between palladium dispersion and activity based on T_{50}. By contrast, a lower temperature of calcination of the perovskite precursor combined to a non reducibility of Fe^{3+} compared to the other B cations were believed to be responsible for such a good activity of $Pd/LaFeO_3$.

This work deals with the catalytic oxidation of chlorobenzene in air over $Pd/LaBO_3$ (B = Co, Fe, Ni, Mn) and a conventional Pd/γ-Al_2O_3 solids. Attention has been particularly paid on the determination of the catalyst surface states from *quasi in situ* XPS studies performed after the successive steps of the process that are calcination, reduction and exposure to the reactive VOC/air atmosphere over $Pd/LaBO_3$ (B = Co, Fe). The main issues to address here is the comprehension of the effect of the hydrogen activation on the catalyst performances of $Pd/LaBO_3$.

2. Experimental

2.1. Catalysts preparation

The perovskites were synthesized following preparation modes given in the literature [7–9]. $LaBO_3$ (B = Co, Fe, Ni) perovskites were prepared from citrate precursors. $La(NO_3)_3{\cdot}6H_2O$ (Fluka, >99%) and B nitrate salts ($Co(NO_3)_2{\cdot}6H_2O$ (Fluka, >98%); $Ni(NO_3)_2{\cdot}6H_2O$ (Prolabo, 98%); $Fe(NO_3)_2{\cdot}9H_2O$ (Fluka, 98%)) were mixed together in a suitable proportion in a minimum of water. A stoichiometric amount of citric acid (CA: Prolabo, >99.7%) ($n_{CA}/(n_B + n_{La}) = 1$) dissolved in water was then added to the resulting solution which was maintained at 100 °C for 12 h. After evaporation under reduced pressure at 70 °C a viscous gel was obtained. It was dried in an oven at 100 °C for 10 h, grounded and finally calcined at 600 °C (B = Fe) or 800 °C (B = Co, Ni) for 5 h. $LaMnO_{3+\delta}$ was prepared according to a Pechini derived method. A suitable amount of $Mn(CH_3CO_2)_2{\cdot}4H_2O$ (Prolabo, 99%) was dissolved in CA with an excess of ethylene glycol (EG: Prolabo, 99.7%) ($(n_{CA}/n_B) = 4$; $n_{EG}/n_{CA} = 1.38$). After evaporation the gel obtained was dried and grounded as above. The solid was finally calcined at 700 °C for 5 h. $Pd/LaBO_3$ were prepared by impregnating the perovskite carrier with an aqueous solution containing the appropriate amount of $Pd(NO_3)_3$ (Alfa Aesar: solution, Pd 8.5%, w/w) in order to reach a palladium loading of 0.5 wt.%. The mixture was submitted to evaporation by means of a rotary evaporator at 50 °C for 2 h. After drying one night at 100 °C, the desired powders were obtained.

2.2. Catalytic activity evaluation

Conversion measurements were carried out in a flow reactor at atmospheric pressure at programmed temperature between room temperature to 530–600 °C (1 °C/min). The amount of loaded catalyst was 0.5 g. Prior to each evaluation, the catalyst was calcined during 4 h in flowing air (2 L/h) at 400 °C, then purged at room temperature with N_2 (4 L/h) for 0.5 h. A reduction was performed under flowing H_2 (2 L/h) from room temperature to 200 °C (1 °C/min), the isotherm being kept for 2 h. After cooling down, the catalyst was swept with N_2 (4 L/h) for 0.5 h. The reactor was then heated up to the final temperature at a rate of 1 °C/min. For activity determination, 1000 ppmv of chlorobenzene in air flowing at 6 L/h was introduced in the reactor. A set of valves allowed by-passing the reactor to lead the feed stream directly into the gas chromatograph sampling loop, which provides a direct measurement of the VOC concentration in the feed. The outlet gas was monitored by using an on-line Varian 3800 chromatograph, equipped with a TCD and a FID. HCl and Cl_2 were both trapped at the exit of the reactor in a bubbler containing an aqueous solution of KI (0.1 M). Polychlorinated compounds were identified both by MS (Omnistar) and by GC by the elution of different standards. Aliquot of the bubbler solution was taken at the beginning of each injection. HCl amount was evaluated from $[H_3O^+]$ determined by pH measurement and the amount of chlorine was evaluated from $[I_3^-]$ determined by visible spectroscopy.

Conversion was calculated according to : α

$$= \frac{n_{CO_2} + 6n_{PhCl_i}}{n_{CO_2} + 6n_{PhCl_i} + 6n_{PhCl}} \times 100$$

When mentioned in the figures CO_x is the summation of CO and CO_2 production and ppm C (B.P) refers to ppm carbon considering only the organic by-products of the reaction.

2.3. Catalysts characterization

Phase analysis was performed by X-ray powder diffraction using a Siemens D5000 or a Huber diffractometer. Crystallites sizes of the perovskites were evaluated by means of the Scherrer equation.

BET surface areas were measured by a single point BET method using a Quantasorb Jr. apparatus. Before experiment, the fresh catalysts were submitted to a flow of nitrogen for 1 h at 120 °C.

Elemental analyses were performed at the "Service Central de Microanalyse" of the CNRS (Vernaison, France). Palladium content determined by plasma emission spectroscopy on catalysts was close to 0.5% for all calcined samples (see Table 1).

Pulse chemisorption measurements were performed using an Altarima AMI-200 apparatus. The calcined samples were pre-treated for 2 h in a flow of hydrogen diluted in Ar (5% H_2/Ar; 30 mL/min) for 2 h. The sample was then exposed to a flow of argon from RT to 400 °C in order to get rid off hydrogen excess for 2 h before to be cooled down to 100 °C. Pulse chemisorption measurements were performed at that temperature with 5% H_2/Ar.

XPS analyses were performed with a VG ESCALAB 220XL spectrometer. The analysis chamber was operated under ultrahigh vacuum with a pressure close to 5×10^{-7} Pa. X-rays were produced by a monochromatized aluminium anode (1486.6 eV) radiation (15 kV, 20 mA). For these measurements, the binding energy (BE) values were referred to the C 1s photopeak at 285 eV. The surface atomic ratios were calculated by correcting the intensity with theoretical sensitivity factors based on the Scofield cross-section. Peak decomposition was performed using the Eclipse software from VG. The following peak intensities were used for the quantitative analysis: Pd 3d, O 1s, Co 2p, C 1s, Fe 3p, La 4p and Cl 2p. The sample was deposited in a glass support. The successive treatments performed on the catalyst were calcination at 300 °C for 1 h in flowing air (2 L/h, 2 °C/min) followed by one night in flowing air at room temperature, reduction at 200 °C for 2 h in flowing H_2 (2 L/h, 2 °C/min) followed by one night in the catalytic chamber, treatment under reactive stream (1000 ppmv PhCl in air, 100 mL/min) from 20 °C to a temperature characteristic of a low PhCl conversion (θ = 230 °C and 280 °C for $Pd/LaFeO_3$ and

Table 1
Characterization of the fresh calcined catalysts

Catalyst	ASA (m^2/g)	Pd (wt.%)	Dispersion (%)	D_c $LaBO_3$ (nm)
$Pd/LaMnO_{3+\delta}$	17 ± 2	0.48	7	20
$Pd/LaFeO_3$	16 ± 2	0.47	19	15
$Pd/LaCoO_3$	5 ± 1	0.41	14	52
Pd/LaNiO	8 ± 1	0.49	–	25

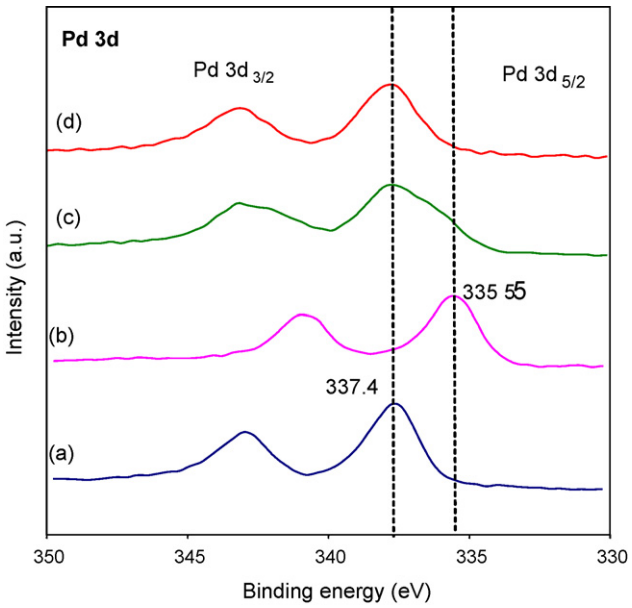

Fig. 1. Evolution of Pd 3d XPS spectrum of $Pd/LaFeO_3$ during the overall process. After (a) calcination, (b) reduction, (c) exposure on stream from RT to 230 °C, (d) exposure on stream from RT to 310 °C.

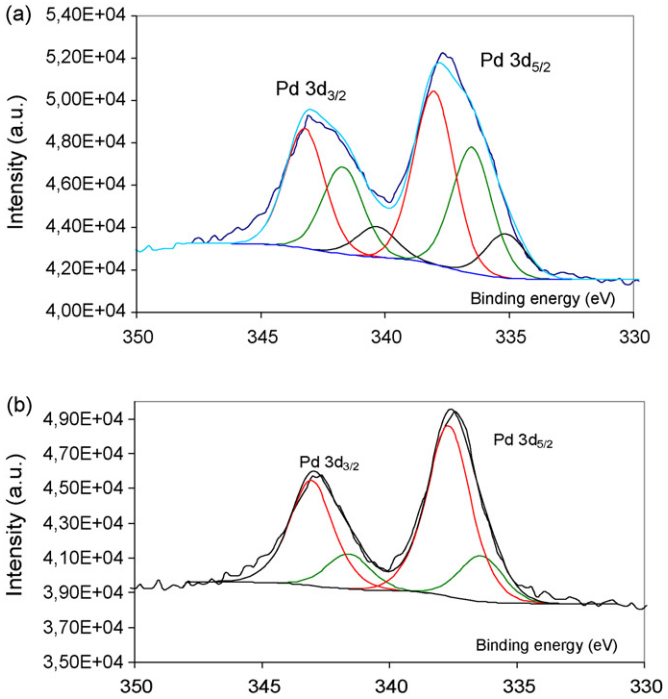

Fig. 2. Decomposition of the Pd 3d XPS spectra of $Pd/LaFeO_3$ after exposure on stream from RT to 230 °C (a) and from RT to 310 °C (b).

$Pd/LaCoO_3$, respectively) or of a high PhCl conversion (θ = 310 °C for $Pd/LaFeO_3$).

Extraction of the Cl 2p XPS signal from the La 4p one was carried out considering ΔE(La $4p_{3/2}$–La $4p_{1/2}$) = 3.3 eV; I(La $4p_{3/2}$)/I(La $4p_{1/2}$) = 2.5 and for the Cl 2p core level ΔE(Cl $2p_{3/2}$–Cl $2p_{1/2}$) = 1.6 eV and I(Cl $2p_{3/2}$)/I(Cl $2p_{1/2}$) = 2.

3. Results

3.1. catalysts characterization

Relevant physical characterizations of the fresh calcined catalysts are reported in Table 1. XRD patterns of the fresh $Pd/LaBO_3$ samples (not shown here) exhibit only the perovskite structure: a rhombohedral phase for $LaCoO_3$, $LaNiO_3$ as for $LaMnO_{3+\delta}$ and an orthorhombic one for $LaFeO_3$, the crystallite sizes ranging from 15 to 52 nm. Apparent surface areas of the catalysts which range between 5 and 17 m^2/g are similar to those of the perovskites. It has been shown from H_2 chemisorption data that the Pd dispersion over perovskite is poor and decreases as follow: $Pd/LaFeO_3$ (D = 19%) > $Pd/LaCoO_3$ (14%) > $Pd/LaMnO_{3+\delta}$ (7%).

3.2. XPS studies

The surface state of the $Pd/LaCoO_3$ and $Pd/LaFeO_3$ samples has been investigated by XPS after each step of the global process of total oxidation of chlorobenzene, that are calcination, reduction and exposure to the reactive atmosphere from room temperature to 280 °C for $Pd/LaCoO_3$ and to 230 and 310 °C for $Pd/LaFeO_3$. The results are displayed in Table 2 and Figs. 1–6.

3.2.1. $Pd/LaFeO_3$

XPS results after calcination and reduction, performed over the same catalysts regarding total oxidation of toluene, have been given elsewhere [8]. To sum up after calcination the Pd $3d_{5/2}$ BE which is at 337.4 eV (Fig. 1) is higher than the usual value of PdO (336.2 eV) [10] and could indicated the formation of oxidized palladium entities in a special environment as for example $Pd^{3+/4+}$ located in the surface B-site of the perovskite network [11]. The XPS atomic Fe/La ratio of 0.84 is slightly lower than the global one. This low Fe/La atomic ratio (Table 2) can be explained by a segregation of La to the surface of the catalyst due to the tendency of La^{3+} cations to react with atmospheric H_2O and CO_2. After treatment with hydrogen palladium (335.5 eV) is reduced to Pd^0 and Fe^{3+} is the only iron species. Exposure of the catalyst surface to the reactive atmosphere from room temperature up to 230 °C results in a significant increase of the XPS Pd $3d_{5/2}$ width signal (FWMH = 3.3 eV), at an apparent maximum at 337.4 eV, which attests of at least two different palladium entities (Fig. 1(c)). Indeed decomposition of the Pd $3d_{5/2}$ envelop reveals three peaks positioned at 338.0, 336.5 and 335.1 eV ascribed to Pd^{x+} ($x \geq 2$), Pd^{2+} and Pd^0, respectively with atomic percentages of 51, 36 and 13%, respectively (Fig. 2a). In the second experiment, increasing the

Table 2
XPS composition of the $Pd/LaBO_3$ (B = Fe, Co) during the overall process

Experimental conditions	XPS composition	
	$Pd/LaCoO_3$	$Pd/LaFeO_3$
Calcination	$LaCo_{0.52}O_{3.04}Pd_{0.098}C_{0.40}$	$LaFe_{0.84}O_{2.5}Pd_{0.05}C_{0.15}$
Reduction	$LaCo_{0.68}O_{2.53}Pd_{0.088}C_{0.40}$	$LaFe_{0.81}O_{2.62}Pd_{0.05}C_{0.58}$
On stream to 280 °C (230 °C*)	$LaCo_{0.66}O_{4.06}Pd_{0.090}C_{0.28}Cl_{0.27}$	$LaFe_{0.79}O_{2.57}Pd_{0.07}C_{0.29}Cl_{0.25}$*
On stream to 310 °C		$LaFe_{0.83}O_{2.25}Pd_{0.05}C_{0.16}Cl_{0.23}$

* Temperature of 230 °C refers to the iron based catalyst (see experimental section part 2.3).

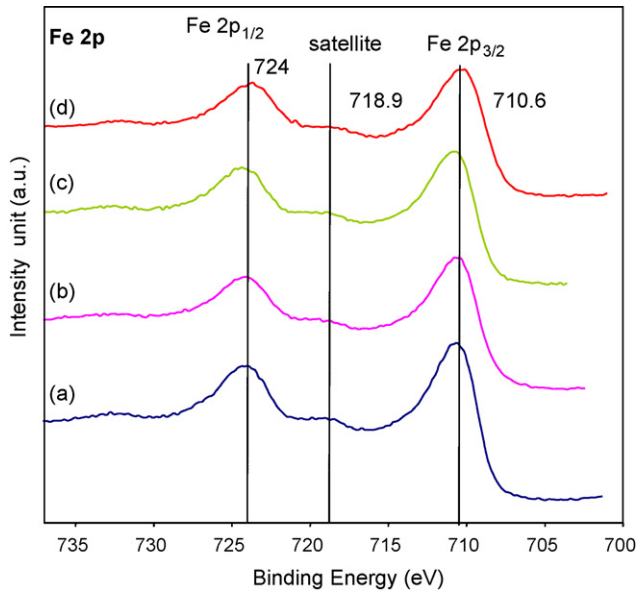

Fig. 3. Evolution of Fe 2p XPS spectrum of $Pd/LaFeO_3$ during the overall process. After (a) calcination, (b) reduction, (c) exposure on stream from RT to 230 °C, (d) exposure on stream from RT to 310 °C.

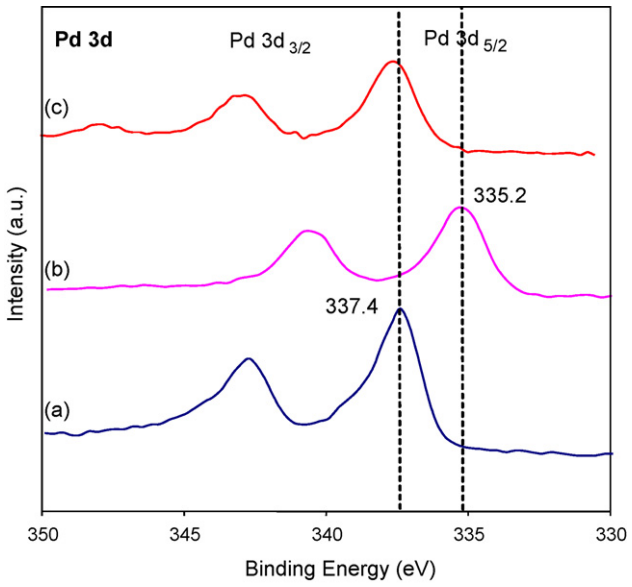

Fig. 5. Evolution of the Pd 3d XPS spectrum of $Pd/LaCoO_3$ during the overall process. After (a) calcination, (b) reduction, (c) exposure on stream from RT to 280 °C.

final temperature of 80 °C, results now in a significant decrease of the XPS FWMH Pd $3d_{5/2}$ signal (2.25 eV) (Fig. 1(d)). Decomposition of the Pd $3d_{5/2}$ envelop shows now only two peaks positioned at 337.7 (Pd^{x+}) and 336.4 eV (Pd^{2+}) with atomic percentages of 61 and 39%, respectively indicating a deeper oxidation/chlorination of the palladium particles since no Pd^0 is seen anymore (Fig. 2b).

The binding energy of Fe $2p_{3/2}$ peak at 710.6 eV associated with a satellite at 8.3 eV upscale confirms the presence of Fe^{3+} (Fig. 3) [12]. It is worth mentioning that the Fe $2p_{3/2}$ BE keeps constant within the margin of error after exposure to the reactive atmosphere as well as the XPS atomic ratio (La/Fe), the value of which keeps equal to 0.81 (±0.03). The Cl 2p XPS signal has also been investigated in order to gain information on the nature and amount of chlorine. As this signal is drown in the La 4p XPS signal, the contribution of the XPS Cl 2p signal to the total one has been carried out by subtraction of the La 4p components (Fig. 4). The BEs of Cl $2p_{3/2}$ positioned at 198.2 eV and 198.4 eV on the spectrum recorded at 230 and 310 °C, respectively attest of Cl^- species [13]. Owing to the uncertainty in the decomposition of the signal, it is not possible to characterize the chlorination site which could be Fe or La, to give $FeCl_3$ (198.3 eV [13]) and/or LaOCl (198.1 eV [14]). Chlorine can also be bound to palladium to form $PdCl_2$ or PdO_xCl_y. In fact the Pd $3d_{5/2}$ component at 337.4 ± 0.3 eV is slightly lower than the one of $PdCl_2$ (BE Pd $3d_{5/2}$ = 337.9 ± 0.3 eV [15] 338.2 eV [16]; with a C1s BE at 285 eV) and probably indicate PdO_xCl_y like species [16] which are associated with a Pd $3d_{5/2}$ BE located between the energy of PdO

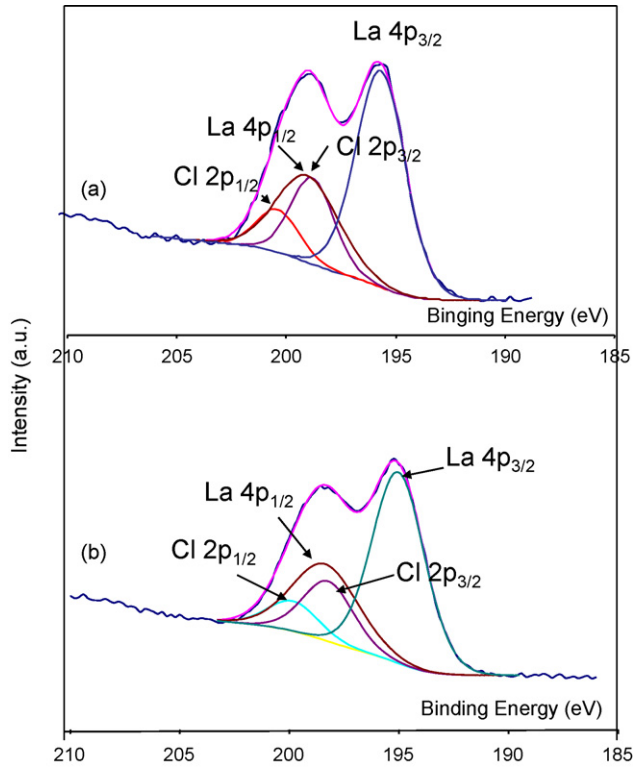

Fig. 4. Decomposition of the La 4p and Cl 2p XPS spectra of $Pd/LaFeO_3$ after exposure (a) on stream from RT to 230 °C, (b) exposure on stream from RT to 310 °C.

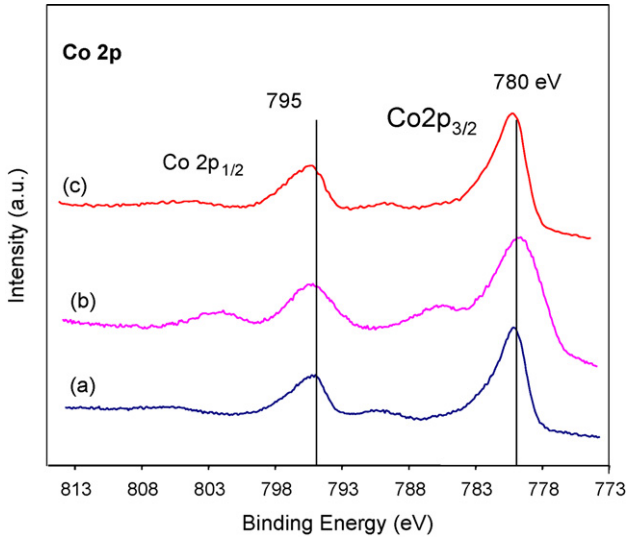

Fig. 6. Evolution of Co 2p XPS spectrum of $Pd/LaCoO_3$ during the overall process. After (a) calcination, (b) reduction, (c) exposure on stream from RT to 280 °C.

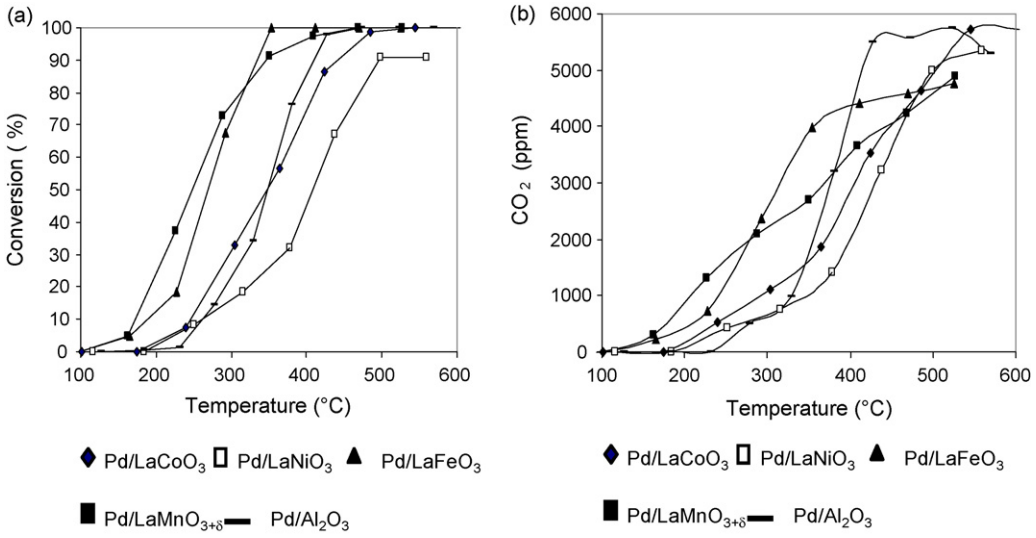

Fig. 7. (a) Curves of conversion of 1000 ppmv chlorobenzene in air over $Pd/LaBO_3$ (B = Co, Mn, Fe) and Pd/Al_2O_3 and (b) of CO_2 formation versus temperature (m_{cat} = 0.5 g; F_{air} = 6 L/h).

(336.2) and $PdCl_2$ (338.2). These species have been claimed elsewhere for platinum [2] to be potential active chlorination sites.

3.2.2. $Pd/LaCoO_3$

To sum up again the previous results [7] after calcination oxidized Pd entities with unusual BE are generated on the perovskite which shows a low Co^{3+}/La^{3+} reflecting a higher segregation of lanthanum at the surface of the catalyst compared with the previous catalyst (Table 2). Metallic palladium is then detected after the hydrogen treatment. In flowing reactive atmosphere at 280 °C, the Pd $3d_{5/2}$ signal centred at 337.6 eV (FWMH of 2.00 eV) can be associated with oxichloride like species (Fig. 5).

The Co 2p XPS spectra are reported in Fig. 6. It must be mentioned that in Fig. 6a the weakness of the shake-up peak associated with the Co $2p_{1/2}$ precludes a significant Co_3O_4 formation [17] and indicates a Co^{3+} presumably located in the B site of the perovskite framework. Reduced cobalt species (Co^{2+}, Co^0) are detected after hydrogen reduction. After exposure to the reactive atmosphere, the global Co 2p envelop (Fig. 6(c)) appears rather similar to that in Fig. 6(a). Hence total reoxidation of the reduced cobalt species occurs accompanied with a surface reconstruction of the perovskite $LaCoO_3$. The XPS Co/La ratio of 0.52 (±0.05) after calcination increases to a value of 0.67 (±0.07) after hydrogen exposure and keeps stable under the reactive stream showing a Co enrichment of the surface during the catalytic test.

The Cl $2p_{3/2}$ component is at 198.8 eV. This value is rather similar to those obtained for the previous catalyst taking into account the margin of error. Additionally the XPS Cl/La ratio of 0.27 which is close to those obtained previously could suggest that the B cation is not the primary site of chlorination.

The $(Pd/La)_{XPS}$ ratios which are related to the surface of the support occupied by palladium are 0.09 (±0.009) and 0.06 (±0.006) for $Pd/LaCoO_3$ and $Pd/LaFeO_3$, respectively. Such ratios depend both on the palladium dispersion and on the specific surface of the support. Hence considering the ratio of the surface areas of the support, this is qualitatively in agreement with the values of the $(Pd/La)_{XPS}$ ratios considering a rather similar palladium dispersion for both samples.

3.3. Catalytic activity

The curves of conversion of PhCl and of production of CO_2 versus temperature over $Pd/LaBO_3$ (B = Fe, Mn, Ni, Co) as well as the one of Pd/Al_2O_3 are given in Fig. 7(a) and (b) and some characteristic parameters of the reaction are reported in Table 3. The onset of conversion of chlorobenzene occurs around 100 °C on $Pd/LaMnO_{3+\delta}$ and $Pd/LaFeO_3$ and around 170–185 °C on $Pd/LaCoO_3$ and $Pd/LaNiO_3$. The catalysts can be ranged by decreasing activity based on T_{50} as follow: $Pd/LaMnO_{3+\delta}$ (243 °C) > $Pd/LaFeO_3$ (270 °C) > $Pd/LaCoO_3$ (360 °C) > $Pd/LaNiO_3$ (408 °C). The same sequence order is kept regarding T_{90} excepted for the two first catalysts where the order is inversed. For each catalyst the higher value of $T_{50(CO_2)}$ (temperature at which 50% of the reactant is converted into CO_2) compared to T_{50} reflects significant production of gaseous by-products and $Pd/LaFeO_3$ appears to be a more efficient catalyst than $Pd/LaMnO_{3+\delta}$.

The curves of PhCl conversions as a function of temperature have been given in Fig. 8 comparatively for $Pd/LaBO_3$ samples and $LaBO_3$. Since substantial amounts of CO have been detected over the perovskites alone (which have not been previously reduced before the catalytic test) the CO_x production curves have also been reported in Fig. 8 where CO_x is the summation of CO and CO_2 production. Let us recall that with palladium based catalysts only CO_2 has been detected. It can be seen that conversion begins at temperatures quite similar (at a higher θ for $LaFeO_3$, but the precursor of the perovskite has been calcined at a higher temperature, see below). A significant difference is the absence of a minimum of conversion in the medium temperature range (200–300 °C) for the palladium-based catalysts, resulting in light-off temperatures substantially lower. The difference in the light-off temperatures between the solids with or without palladium is clearly more important for $LaMnO_{3+\delta}$ (158 °C) than the Ni and Co

Table 3
Activity of the $Pd/LaBO_3$ catalysts for the total oxidation of PhCl (1000 ppmv PhCl–air F/w = 220 NmL/(min g))

Catalyst	VVH (h^{-1})	T_{50} (°C)	T_{90} (°C)	$T_{50(CO_x)}$ (°C)	$T_{90(CO_x)}$ (°C)
$Pd/LaMnO_{3+\delta}$ (700[a])	17,800	243 (401[b])	342	366 (441[b])	–
$Pd/LaCoO_3$ (800)	7,500	360 (306)	442	400 (422)	–
$Pd/LaFeO_3$ (600)	10,500	270 (464)	335	318 (478)	–
$Pd/LaNiO_3$ (800)	2,300	408 (460)	493	428 (490)	–
Pd/Al_2O_3	11,700	348	395	370	–

[a] Temperature of calcination of the precursor of the perovskite.
[b] Characteristic temperatures of the perovskite alone.

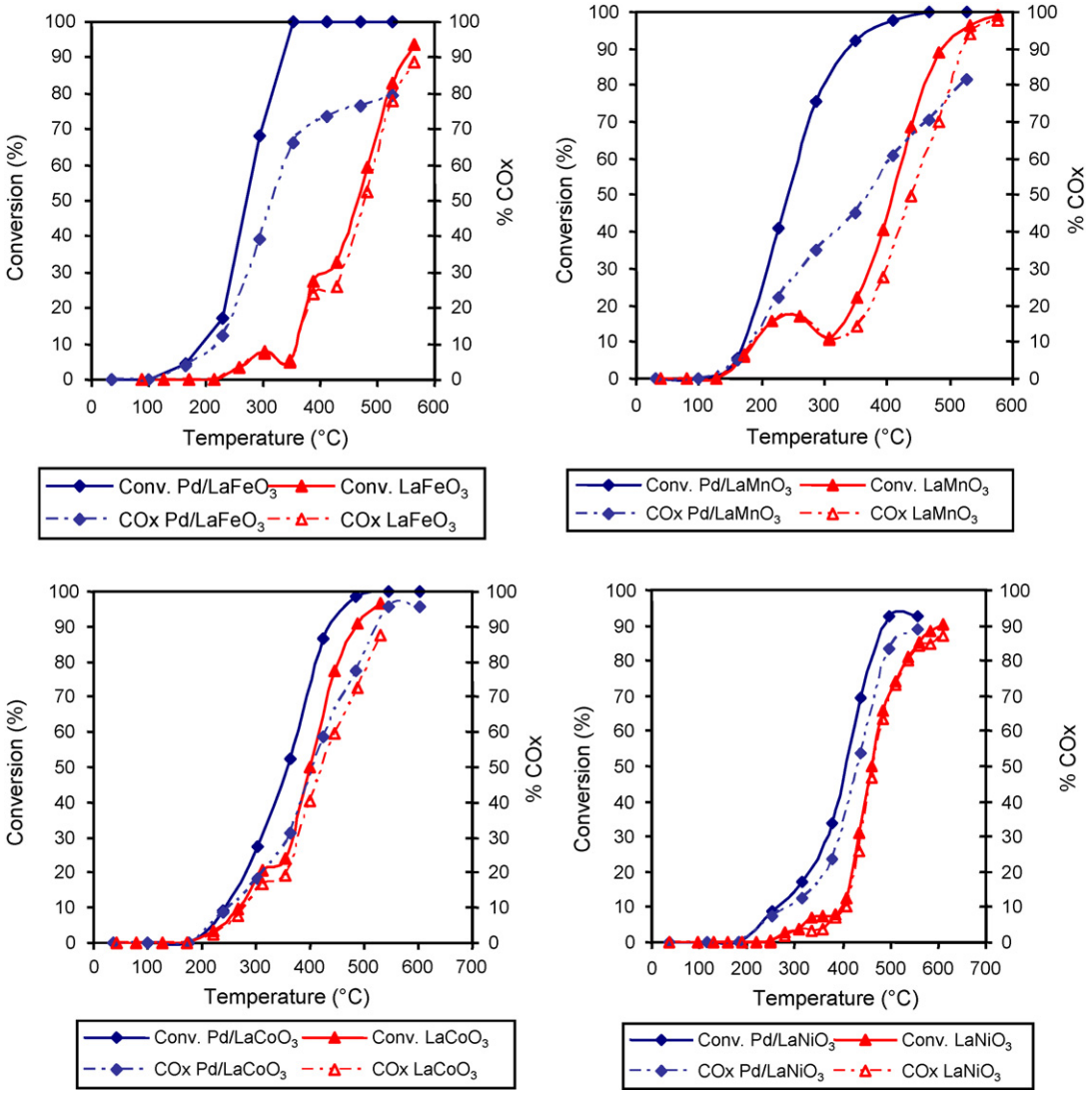

Fig. 8. Comparison of the conversion and CO_x formation on $LaBO_3$ and $Pd/LaBO_3$ (B = Fe, Mn, Co, Ni)–1000 ppmv PhCl; F/w = 220 NmL/(min g).

based perovskites (52 and 36 °C, respectively). The difference of 194 °C for the iron based catalysts $LaFeO_3$ will be not discussed as the precursor of the perovskite used for the impregnation by the palladium salt has been calcined at a lower temperature (600 °C against 700 °C) which results in an increase of the apparent surface area (18 against 7 m^2/g). We had previously attributed the decrease of the conversion with temperature observed on the perovskite alone to the consumption of reactive oxygen entities of the perovskite with an incomplete reoxidation by O_2 [17]. The absence of such a decrease can be explained by a catalytic effect of palladium on the perovskite reoxidation, which refills faster the oxygen vacancies in reactive oxygen entities able to keep converting the chlorobenzene.

Here only CO_2 as oxygenated compound of carbon is detected contrarily to the perovskites where CO is observed. This is in line with the well-known good activity of palladium in the $CO + 1/2\ O_2 = CO_2$ reaction. However, it must be stressed that the differences between the T_{50} and $T_{50\,(CO_x)}$ are higher for the palladium based catalysts than for the perovskites alone showing that by-product formation increases with palladium. Indeed a significant production of polychlorinated benzenes and of perchloroethylene (PCE) has been shown. The concentrations of PhCl, CO_2, of the different by-products (expressed in ppm C) and of total carbon versus temperature are given in Fig. 9. It is noticed that the polychlorinated by-products can amount up to about 30% of the initial input of PhCl.

The concentrations of HCl, Cl_2 and polychlorinated by-products (PhCl and C_2Cl_4) as the total chlorine content (ppm Cl) as a function of temperature are reported in Fig. 10. A chlorine deficit is observed from room temperature to 350 °C, indeed to higher temperatures regarding $Pd/LaCoO_3$ and $Pd/LaNiO_3$ which probably indicates that a substantial fraction of chlorine is bound to the catalyst surface. The polychlorobenzenes begin to be detected around 150–250 °C to reach a maximum production at about 350–450 °C. When the chlorobenzene is totally converted, the production of polychlorinated compounds starts to decrease and at that stage hydrogen chloride and dichlorine begin to be detected. Beyond the maximum of polychlorobenzenes production, oxidation of the chloroaromatics prevails over the chlorination either because of an increase of temperature favours the oxidation of chlorobenzene as compared to its chlorination, or simply because the oxidation rates of polychlorobenzenes are higher than that of their formation. The second explanation appears to be more likely since the fraction

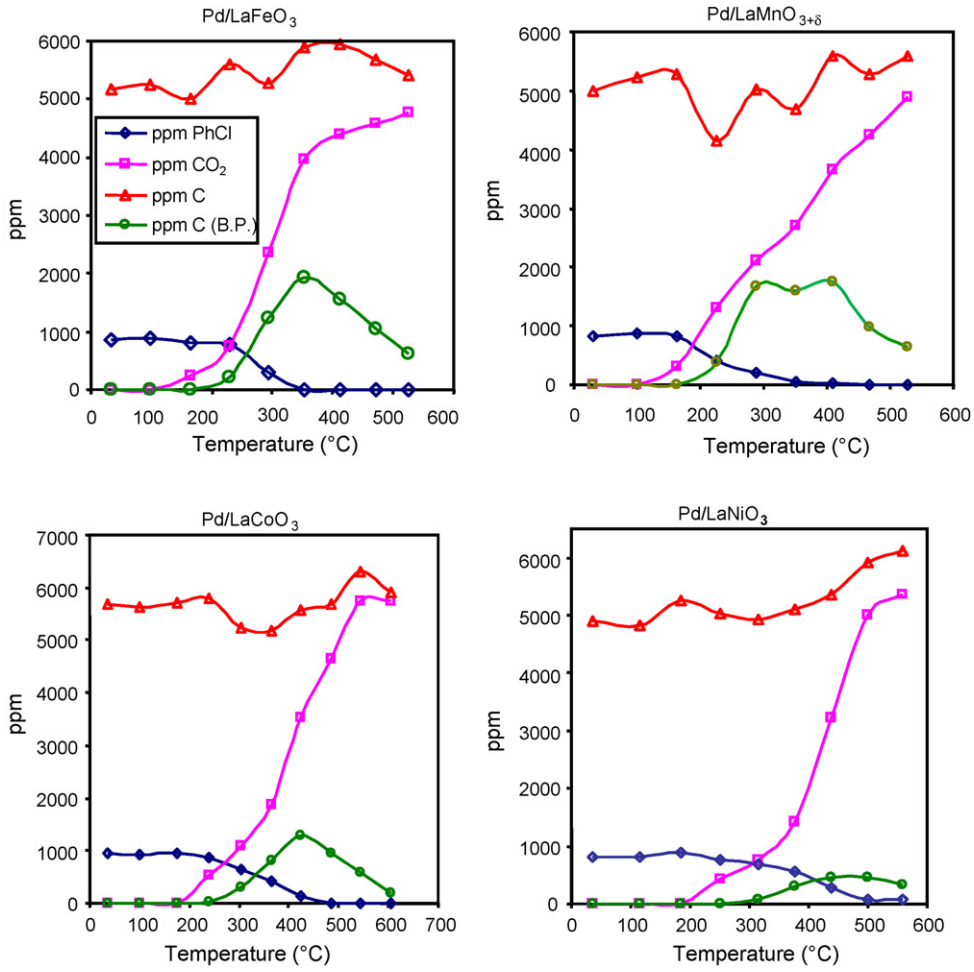

Fig. 9. Evolution of CO_2, PhCl and $PhCl_x$, C total (ppm C) in function of the temperature on $Pd/LaBO_3$ (B = Mn, Co, Fe, Ni).

of polychlorobenzenes begins to decrease only when 100% PhCl conversion is achieved.

The total spectrum of the congeners $PhCl_x$ (x = 2–6) and of C_2Cl_4 during the course of the reaction has been established. The concentration profiles of total chlorine (ppm Cl) arisen from the polychlorobenzenes production as a function of temperature are given in Fig. 11. The maxima of production are at 370, 409, 450 and 500 °C, respectively for B = Fe, Mn, Co and Ni.

The isomers distribution of the congeners $PhCl_x$ (x = 2–4) as a function of temperature is given in Fig. 12 and the results are reported in Table 4. The dichlorobenzenes are first detected, and appear by decreasing amounts: 1,2-$PhCl_2$ > 1,4-$PhCl_2$ > 1,3-$PhCl_2$, excepted for $Pd/LaFeO_3$, where 1,2-$PhCl_2$ ≈ 1,4-$PhCl_2$ > 1,3-$PhCl_2$; then the trichlorobenzenes are detected, the isomer fraction decreasing owing: 1,2,4-$PhCl_3$ > 1,2,3-$PhCl_3$ > 1,3,5-$PhCl_3$. Regarding the tetrachlorobenzene production, one detects 1,2,3,4-$PhCl_4$ and a composite peak composed of 1,2,4,5-$PhCl_4$ and 1,2,3,5-$PhCl_4$ non separated. $PhCl_5$ and $PhCl_6$ are also detected but in a significantly lower amount that the three other congeners. The succession of $PhCl_x$ production maxima is characteristic of

Table 4
Maximum production of the by-products at θ_{max} of the congener production

Catalyst	$Pd/LaCoO_3$	$Pd/LaMnO_{3+\delta}$	$Pd/LaFeO_3$	$Pd/LaNiO_3$
$PhCl_2$	θ_{max}: 424 °C	θ_{max}: 288 °C	θ_{max}: 293 °C	θ_{max}: 438 °C
m-$phCl_2$ (ppm)	25 (44%)	20 (45%)	29 (47%)	18 (48%)
p-$phCl_2$ (ppm)	31 (56%)	34 (55%)	32 (53%)	20 (52%)
o-$phCl_2$ (ppm)	72	121	73	26
$PhCl_3$	θ_{max}: 424 °C	θ_{max}: 409 °C	θ_{max}: 354 °C	θ_{max}: 499 °C
1,3,5-$phCl_3$ (ppm)	2	11	9	3
1,2,4-$phCl_3$ (ppm)	39	65	65	11
1,2,3-$phCl_3$ (ppm)	20	41	32	5
$PhCl_4$	θ_{max}: 485 °C	θ_{max}: 409 °C	θ_{max}: 354 °C	θ_{max}: 499 °C
1,2,4,5-$phCl_4$ (ppm), 1,2,3,5-$phCl_4$ (ppm)	17	33	66	2
1,2,3,4-$phCl_4$ (ppm)	12	20	31	1
$PhCl_5$ (ppm)	27 (θ_{max}: 545 °C)	32(θ_{max}: 527 °C)	80 (θ_{max}: 411 °C)	1 (θ_{max}: 559 °C)
$PhCl_6$ (ppm)	6 (θ_{max}: 606 °C)	4 (θ_{max}: 527 °C)	2 (θ_{max}: 354 °C)	1 (θ_{max}: 499 °C)

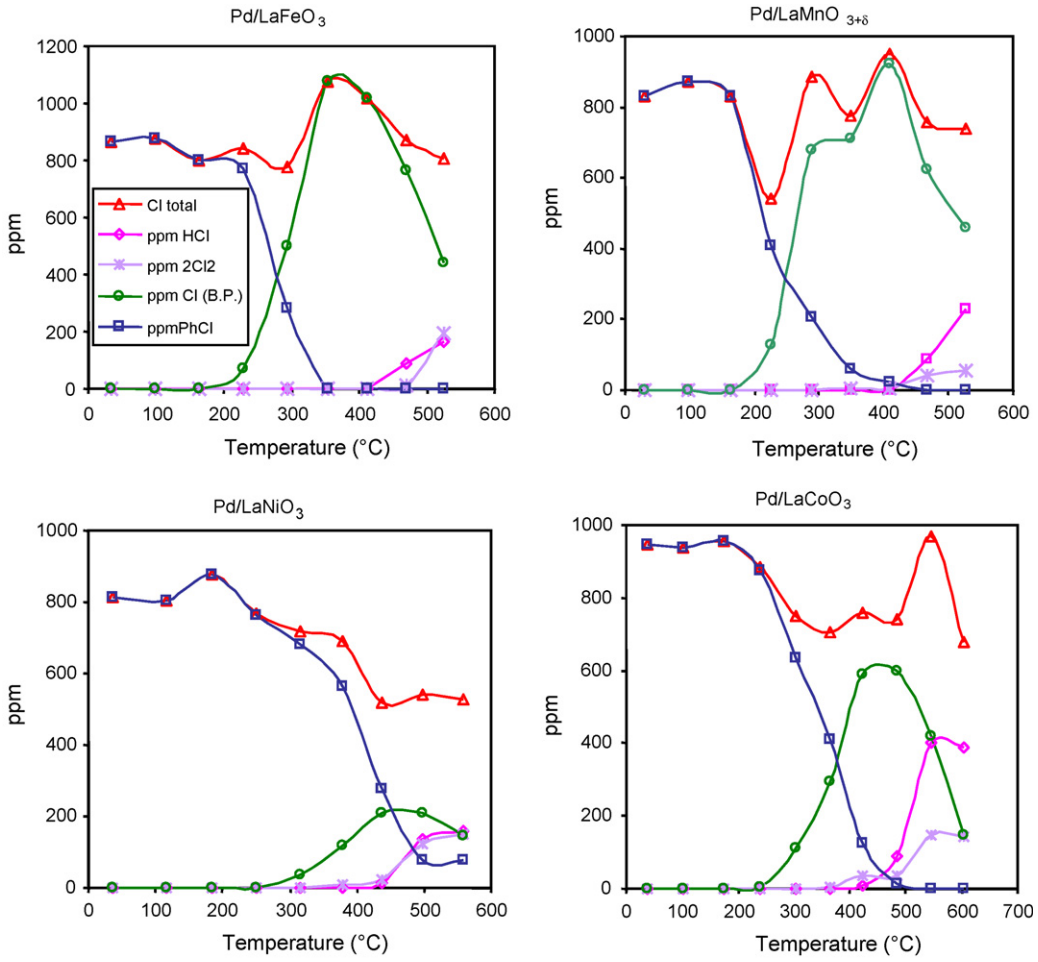

Fig. 10. Evolution of PhCl, HCl, Cl_2, $PhCl_x$ and C_2Cl_4, Cl total (ppm Cl) in function of the temperature on $Pd/LaBO_3$ (B = Mn, Co, Fe, Ni).

successive chlorination reactions. Furthermore the isomer distribution with a substitution on the aromatic ring in *ortho* and *para* positions is well characteristic of electrophilic substitution on aromatic compounds. Hence here the formation of the different polychlorobenzenes is consistent with a kinetic of successive reactions of electrophilic substitution of H by Cl on the aromatic ring. The formation of C_2Cl_4 on each catalyst is also detected from around 350–400 °C to the end of the reaction (Fig. 12).

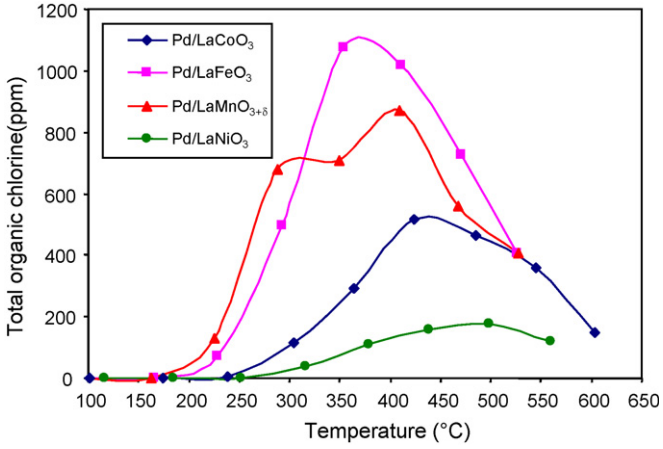

Fig. 11. Total organic chlorine in function of temperature for the catalysts supported on $LaBO_3$ (B = Mn, Co, Fe, Ni).

The amount of polychlorinated compounds is significantly much higher than on the perovskites alone. This clearly indicates an increase of the number of acid sites or of their strength due to the presence of palladium.

For comparison purposes the light-off curves of chlorobenzene and those of CO_2 production as a function of temperature on Pd/Al_2O_3 which has been calcined at 500 °C before the hydrogen treatment are presented in Fig. 7 and the characteristic temperatures are given in Table 3. The conversion of chlorobenzene is characterized by a T_{50} value of 348 °C which is lower than those of $Pd/LaCoO_3$ (T_{50} = 360 °C) and $Pd/LaNiO_3$ (T_{50} = 408 °C) but higher than those of $Pd/LaMnO_{3+\delta}$ (243 °C) and $Pd/LaFeO_3$ (270 °C). The same sequence being respected with T_{90} values. The mass balance for carbon and chlorine look like similar to those reported earlier. A chlorine deficit is observed on the course of the reaction and suggests that chlorobenzene is adsorbed on the support. The polychlorinated compounds are detected with a similar distribution as above. The temperatures associated with the maximum of the different $PhCl_x$ production are 375 °C (x = 2), 418 °C (x = 3–5) and 535 °C (x = 6) (Fig. 13). The amount of polychlorinated by-products formed on $Pd/\gamma\text{-}Al_2O_3$ is of the same order than those on $Pd/LaBO_3$ which shows that acidic sites are probably associated with Pd^{x+} which has been detected by XPS. The Cl_2 formation is here ascribed to the catalytically activated Deacon reaction by Pd.

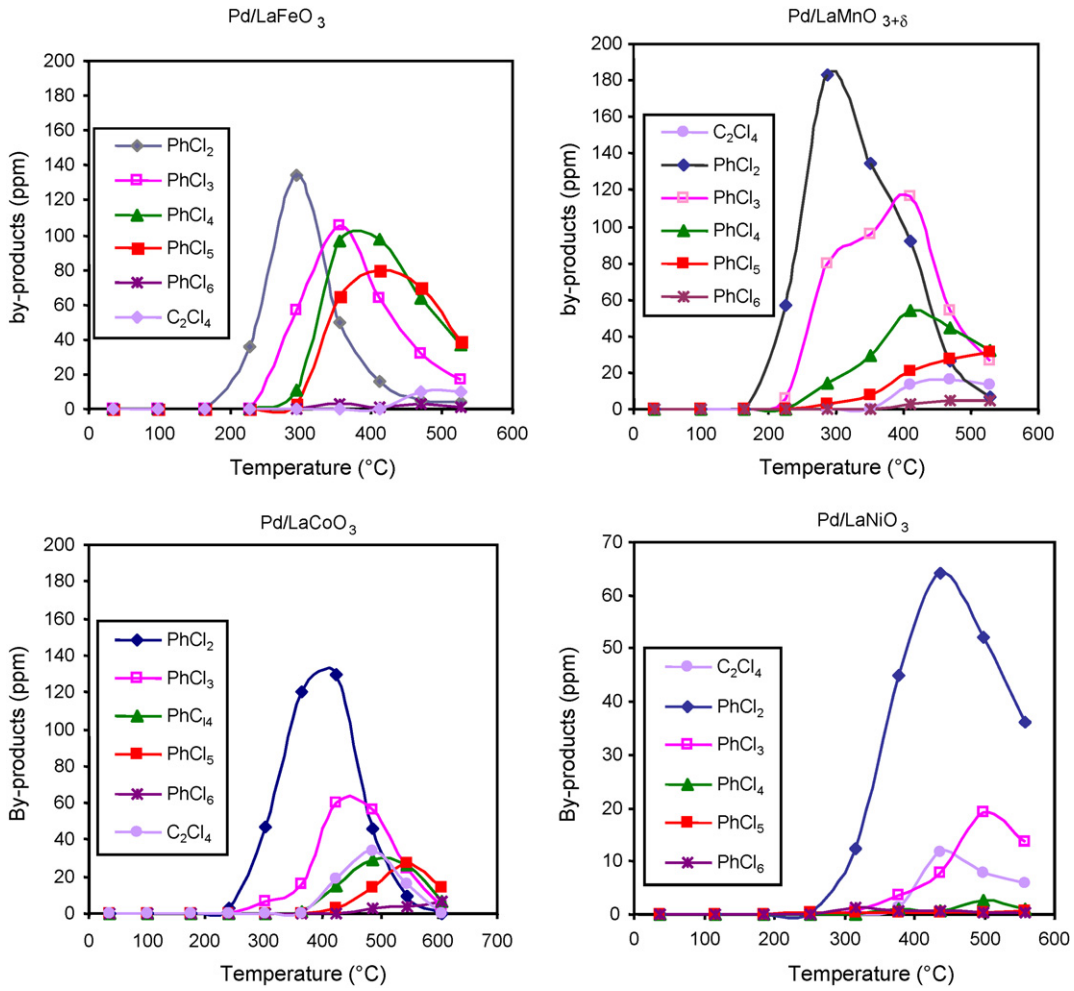

Fig. 12. Distribution of the different congeners in function of temperature for $Pd/LaBO_3$ catalysts.

3.4. Characterization after catalytic test

In Table 5 the Pd and Cl elemental analyses results are reported. The increasing propensity of the catalysts to retain chlorine at the catalyst surface is: $Pd/LaFeO_3 < Pd/LaCoO_3 \approx Pd/LaNiO_3 < Pd/LaMnO_{3+\delta}$. The weight percentages of palladium reveal no significant loss of the active phase during the catalytic testing.

The XRD patterns of the used catalysts are given in Fig. 14. While the perovskite phase is only detected for $Pd/LaFeO_3$ and $Pd/LaMnO_{3+\delta}$, for the two other samples, besides the lines of the initial perovskite phase are additionally detected others which have been assigned to one suboxide of the B cation, namely Co_3O_4 (B = Co) and NiO (B = Ni), and to LaOCl.

4. Discussion

Previous work with $LaBO_3$ (B = Mn, Co, Fe, Ni) has indicated that $LaMnO_{3+\delta}$ and $LaCoO_3$ showed good activities compared to $LaFeO_3$ and $LaNiO_3$ which were poorly active for the catalytic oxidation of chlorobenzene [7]. On time on stream the bulk structure of $LaMnO_{3+\delta}$ and $LaFeO_3$ was preserved while those of $LaCoO_3$ and $LaNiO_3$ decomposed to give LaOCl and suboxides of the B metal. Screening of the palladium based perovskites was here conducted in similar experimental conditions, excepted that the catalysts were pre-reduced. Before to look at catalytic results the effect of

Table 5
Elemental analyses of the used catalysts

Catalyst	Cl (wt.%)	Pd (wt.%)
$Pd/LaMnO_{3+\delta}$	2.20	0.48
$Pd/LaFeO_3$	0.62	0.47
$Pd/LaCoO_3$	1.6	0.41
$Pd/LaNiO_3$	1.73	0.49

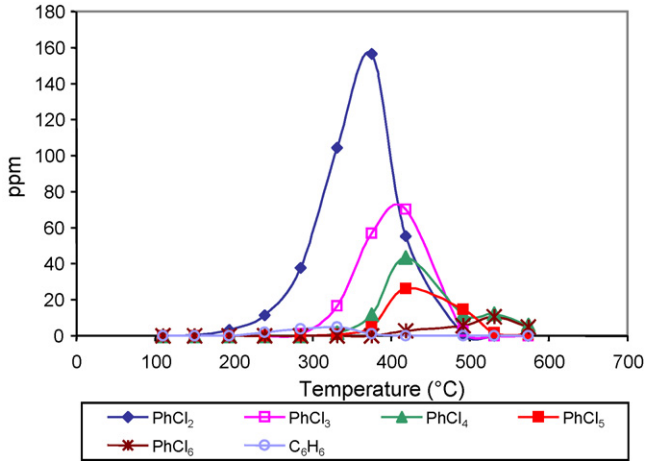

Fig. 13. $PhCl_x$ (x = 2–6) formation in function of temperature for $Pd/\gamma\text{-}Al_2O_3$.

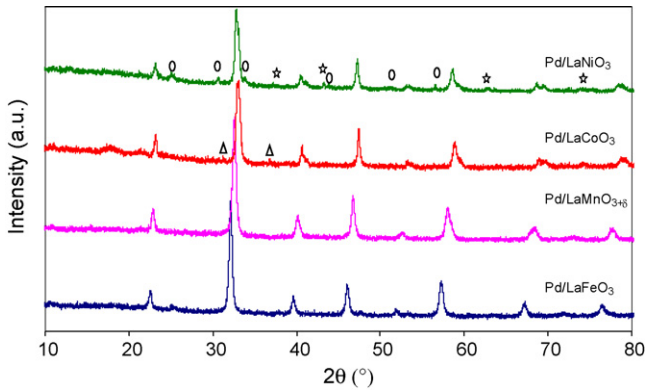

Fig. 14. XRD patterns of the used $Pd/LaBO_3$ catalysts, ○: LaOCl, ☆: NiO; Δ: Co_3O_4.

how the hydrogen treatment can affect the catalyst surface and how this resulting surface behaves on time on stream will be discuss first for the ferrite and cobaltite based catalysts.

XPS results have shown that a treatment with H_2 at 200 °C allows to get palladium at the metallic state accompanied with or not a partial reduction of the B cation of the perovskite (Co^{3+} is transformed into Co^{2+} and Co^0 whereas Fe^{3+} is inert). For both catalysts the palladium particles progressively oxidized and chlorined during the catalytic test into presumably oxide and chloride and more probably (oxy)chloride palladium species. For $Pd/LaFeO_3$ the detection of a mixture of Pd^0–Pd^{x+} at 230 °C indicates that the palladium particles have a metallic core which is progressively covered with PdOxCly layers. The detection of only Pd^{x+} at 310 °C is in line with the extent of palladium (oxi)chlorination. The $LaFeO_3$ network is preserved due to the non reactivity of the Fe^{3+} cation. Regarding now $Pd/LaCoO_3$, it has been shown that the reduced cobalt entities are oxidized on stream. A reconstruction of the perovskite is postulated as the Co2p XPS spectrum is similar as that after calcination. Nevertheless traces of Co_3O_4 and LaOCl detected by XRD reveal an onset of destruction the $LaCoO_3$ lattice as previously reported in the literatures [18,19].

Here the hydrogen pretreatment is expected to have different effects on the perovskite network according to the B cation. Clearly there are three possibilities.

First, the B^{4+} cation is partially reduced inducing a perovskite transformation which is reversible. That is the case of the Mn^{4+} cation which is reduced into Mn^{3+} to give presumably a $LaMnO_3$ phase which transforms back on stream to $LaMnO_{3+\delta}$.

Second, the cation B^{3+} (Co^{3+}, Ni^{3+}) can be reduced to a mixture of B^{2+} and B^0. This is expected to transform the perovskite network (B^{2+}) and to lead to its destruction (B°). By exposure to the oxidative atmosphere $LaBO_3$ is expected to be reconstructed and B^0 can reinsert the cationic vacancies or be oxidized in B_xO_y (Co_3O_4 and NiO for Co and Ni). Hence in that case an irreversible partial destruction of the perovskite is observed.

Third, the B^{3+} cation is unaffected by the hydrogen treatment which is the case for Fe^{3+}.

Hence in the reactive atmosphere, Pd^0 is progressively (oxi)chlorined while the perovskite network is reconstructed with or without its partial destruction.

Considering the catalytic results it has been shown that the palladium-based perovskites exhibit a higher conversion for the total oxidation of chlorobenzene with respect to the perovskites. This indicates the beneficial effect of palladium. However, Pd is not the one to play a role in the reaction as there is no clear relationship between the palladium dispersion and activity. Hence it is clear that the perovskite played a role in the reaction.

The different results have been explained in the light of a kinetic scheme already exposed for $LaBO_3$ which has been slightly modified in order to take into account of the presence of palladium.

The reaction scheme for $LaBO_3$ which we have proposed occurs in two steps with a mechanism of Mars and van Krevelen [20]. It is likely the mobile oxygen species which play a role in the oxidation of the VOC following the scheme:

$$\ll O \gg + VOC \rightarrow VOC_{ox} + \ll \square \gg \quad (1)$$

where $\ll O \gg$ and $\ll \square \gg$, respectively stand for a mobile oxygen and an oxygen vacancy. The oxidation of partially oxidized VOC (VOC_{ox}) could proceed, either by other $\ll O \gg$ species or by O_2, while the oxygen vacancies will be refilled by O_2 owing to:

$$\ll \square \gg + O* \rightleftarrows \ll O \gg \quad (2)$$

hence palladium could intervene in the first reaction in a better activation of VOC and in the second reaction by assisting dioxygen dissociation owing to:

$$O_2 + 2* \rightleftarrows 2O*$$

where * is a palladium site, $\ll O \gg$ an active oxygen species of the perovskite and $\ll \square \gg$ is an oxygen vacancy of the perovskite. This scheme accounts for the better activities and the disappearance of the minimum of conversion as a function of temperature over palladium based catalysts. Hence a better apparent surface area of the $Pd/LaFeO_3$ catalyst combined to better palladium dispersion is expected to give more mobile oxygen available. Additionally the partial destruction of the cobaltite network after the hydrogen treatment is expected to alter its oxygen mobility thus reducing the activity of $Pd/LaCoO_3$.

The rate of chlorobenzene destruction into CO_2 reflected by $T_{50\,CO_2}$ values (temperature at γ which 50% of chlorobenzene is converted into CO_2) was found to follow the order: $Pd/LaFeO_3 > Pd/LaMnO_{3+\delta} > Pd/Al_2O_3 > Pd/LaCoO_3 > Pd/LaNiO_3$. It is the same order at low temperature. Hence if $Pd/LaMnO_{3+\delta}$ is the most active catalyst for the global reaction (oxidation and chlorination), $Pd/LaFeO_3$ is the most efficient catalyst. Considering that the PhCl chorination seems to be of the same extent on $Pd/LaMnO_{3+\delta}$ and $Pd/LaFeO_3$ as shown by the $PhCl_x$ production as a function of the temperature (see Fig. 8), on the other hand the oxidation rate is higher for $Pd/LaFeO_3$ than $Pd/LaMnO_{3+\delta}$ contrarily to the perovskite alone. It is suggested that a better dispersion of palladium in lowering the palladium size increases the interface between the palladium and lanthanum ferrite and allows a faster refilling of the oxygen vacancies.

It must be mentioned that all the curves of chlorobenzene conversion relative to Pd/perovskite catalysts rise slowly with temperature compared to the related curve of chlorobenzene conversion on Pd/Al_2O_3 so that at a higher conversion, Pd/Al_2O_3 is more active than $Pd/LaNiO_3$ and $Pd/LaCoO_3$. As the palladium is assisted by the perovskite for the total oxidation of chlorobenzene there is a synergetic effect at low temperature which explains the best activities of the $Pd/LaNiO_3$ and $Pd/LaCoO_3$ samples compared to the Pd/Al_2O_3 one. As the temperature is raised such a synergetic effect is lost as a consequence of the perovskite framework ($LaNiO_3$, $LaCoO_3$) reduction.

Hence a better conversion can be achieved on the perovskite supported palladium compared to the reference $Pd/\gamma Al_2O_3$ if the synergetic effect between palladium and the perovskite is preserved in the course of the reaction.

A direct comparison of the PhCl chlorination rates between the perovskites and the related Pd-based catalysts shows that the active sites are mainly related to the noble metal as PdO_xCl_y. Large amounts of polychlorinated compounds and of C_2Cl_4 in the temperature range of 300–580 °C are observed with a maximum of

about 30% of the initial VOC content. The main route of chlorination of chlorobenzene occurs via consecutive reactions of hydrogen electrophilic substitution on the aromatic ring by chlorine to give $PhCl_x$ species ($x = 2$–6) or by transchloration reactions. The minority route would be the chlorination of absorbed carbon species resulting from the cleavage of the aromatic ring by cracking to give C_2Cl_4.

5. Conclusion

The catalytic performances of the pre-reduced $Pd/LaBO_3$ (B = Co, Mn, Fe) catalysts have been investigated for the total oxidation of 1000 ppmv of chlorobenzene with air. The results have been interpreted in light of the *quasi in situ* XPS studies performed after each step of the process for $Pd/LaCoO_3$ and $Pd/LaCoO_3$. As palladium is totally reduced in hydrogen, the perovskite network is either unaffected or transformed with or without partial destruction. In the reactive atmosphere, Pd^0 is progressively (oxi)chlorined while the perovskite network is reconstructed with or without production of LaOCl and B suboxide. The pre-reduced $Pd/LaBO_3$ samples are more active than the perovskite alone for PhCl oxidation but substantially increase the chlorination rate of PhCl. Among the different catalysts $Pd/LaFeO_3$ shows the best compromise between PhCl oxidation and chlorination rates.

Acknowledgements

We thank the European community through an Interreg 3 France-Wallonie-Flandre project and also IRENI (Institut de Recherches et Environnement Industriel) for financial supports.

References

[1] J.J. Spivey, Ind. Eng. Res. 26 (1987) 2165.
[2] R.W. van den Brink, P. Mulder, R. Louw, Catal. Today 16 (1998) 219.
[3] R.W. van den Brink, M. Krzan, M.M.R. Feijen-Jeurissen, R. Louw, P. Mulder, Appl. Catal. B: Environ. 24 (2000) 255.
[4] R.W. van den Brink, R. Louw, P. Mulder, Appl. Catal. B.: Environ. 25 (2000) 229.
[5] P. Granger, L. Delannoy, J.J. Lecomte, C. Dathy, H. Praliaud, L. Leclercq, G. Leclercq, J. Catal. 207 (2002) 202.
[6] L.G. Tejuca, G. JL, J.M.D. Fierro, Tascon in Advances in Catalysis, vol. 36, Academic Press, New York, 1989, p. 237.
[7] J.-M. Giraudon, A. Elhachimi, F. Wyrwalski, S. Siffert, A. Aboukaïs, J.-F. Lamonier, G. Leclercq, Appl. Catal. B: Environ. 75 (2007) 157.
[8] S. Irusta, M.P. Pina, M. Menedez, J. Santamaria, J. Catal. 179 (1998) 400.
[9] M.P. Pechini, US Patent 330,697 (1967).
[10] D. Briggs, M.P. Seah, Practical Surface Analysis, 2nd ed., John Wiley, Chichester, 1993.
[11] M. Uenishi, M. Taniguchi, H. Tanaka, M. Kimura, Y. Nishihata, J. Mizuki, T. Kobayashi, Appl. Catal. B: Environ. 57 (2005) 267.
[12] M.R. Goldwasser, M.E. Rivas, M.L. Lugo, E. Pietri, J. Perez-Zurita, M.L. Cubeiro, A. Griboval-Constant, G. Leclercq, Catal. Today 107 (2005) 106.
[13] C.D. Wagner, W.M. Riggs, L.E. Davis, J.F. Mulder, in: G.E. Muilenberg (Ed.), Handbook of X-ray Photoelectron Spectroscopy, PerkinElmer Corporation, Eden Prairie, 1978.
[14] G. Sinquin, C. Petit, J.P. Hindermann, A. Kiennemann, Catal. Today 70 (2001) 183.
[15] G. Kumar, J.R. Blackburn, M.M. Jones, R.G. Albridge, W.E. Moddeman, Inorg. Chem. 11 (1972) 296.
[16] A.D. Guimaraes, L.C. Dieguez, M. Schmal, Ann. Brezilian Acad. Sci. 76 (2004) 825.
[17] J.P. Bonnelle, J. Grimblot, A. D'Huysser, J. Electron Spectrosc. Relat. Phenom. 7 (1975) 151.
[18] J.-M. Giraudon, A. Elhachimi, T.B. Nguyen, F. Wyrwalski, S. Siffert, J.-F. Lamonier, G. Leclercq, XX SICAT, Simposio Ibero-Americano de Catalise, Proceeding, Gramado, Brazil, 2006.
[19] G. Sinquin, C. Petit, J.P. Hindermann, A. Kiennemann, Catal. Today 54 (1999) 107.
[20] P. Mars, D.W. Krevelen, Chem. Eng. Sci. 3 (1954) 41.